
FreeVPS: Repurposing Training-Free SAM2 for Generalizable Video Polyp Segmentation

Qiang Hu¹, Ying Zhou¹, Gepeng Ji^{2†}, Nick Barnes², Qiang Li¹, Zhiwei Wang^{1†}

¹Huazhong University of Science and Technology ²Australian National University
zwwang@hust.edu.cn

[†]Corresponding Author

Abstract

Existing video polyp segmentation (VPS) paradigms usually struggle to balance between spatiotemporal modeling and domain generalization, limiting their applicability in real clinical scenarios. To embrace this challenge, we recast the VPS task as a *track-by-detect paradigm* that leverages the spatial contexts captured by the image polyp segmentation (IPS) model while integrating the temporal modeling capabilities of segment anything model 2 (SAM2). However, during long-term polyp tracking in colonoscopy videos, SAM2 suffers from error accumulation, resulting in a snowball effect that compromises segmentation stability. We mitigate this issue by repurposing SAM2 as a video polyp segmenter with two training-free modules. In particular, the intra-association filtering module eliminates spatial inaccuracies originating from the detecting stage, reducing false positives. The inter-association refinement module adaptively updates the memory bank to prevent error propagation over time, enhancing temporal coherence. Both modules work synergistically to stabilize SAM2, achieving cutting-edge performance in both in-domain and out-of-domain scenarios. Furthermore, we demonstrate the robust tracking capabilities of FreeVPS in long-untrimmed colonoscopy videos, underscoring its potential reliable clinical analysis.

1 Introduction

Colonoscopy, the gold standard [1] for the detection of colorectal cancer, employs a mini endoscope to visualize the interior of the lower digestive tract, facilitating inspection and intervention pipelines. Accurate polyp identification is crucial during this procedure, yet endoscopists' differing experience can lead to misdiagnoses [2]. Recently, the emergence of intelligent analysis in colonoscopy [3] has gained wide attention, such as segmenting polyps from images [4–8]/videos [9–12]. These methods hold substantial promise in reducing diagnostic variability, improving polyp detection rates, and providing reliable assessments, thus enhancing procedural precision and patient outcomes.

Despite these successes, we observe a negative correlation between spatiotemporal modeling and domain generalization in current approaches for video polyp segmentation (VPS). The left part of Fig. 1 illustrates that the VPS model (SALI [12]) achieves a higher Dice score of 0.866 in in-domain (ID) scenarios, surpassing the image polyp segmentation (IPS) model QueryNet [8], which scores 0.822 in a per-frame inference manner. However, this advantage unexpectedly reverses under out-of-domain (OOD) conditions, where QueryNet overtakes SALI with better generalizability and experiences less performance degradation (IPS: -35.3% vs. VPS: -41.3%). Given such a **cross-domain degradation** phenomenon, a natural question arises: “How can spatiotemporal modeling and domain generalization be effectively balanced in real clinical scenarios?”

To answer this question, we recast the VPS task into a *track-by-detect paradigm* [13, 14], where polyps are first segmented independently in each frame and then associated across frames to produce

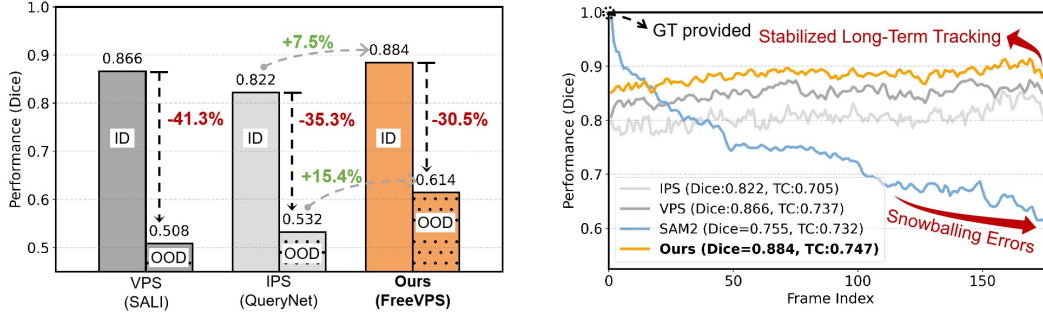


Figure 1: **(Left) Cross-domain degradation.** VPS model (SALI [12]) outperforms IPS model (SALI [12]) in ID scenarios yet lags behind in OOD scenarios. By integrating QueryNet with the proposed FreeVPS, we boost both ID and OOD performance by 7.5% and 15.4%, respectively, with less ID-to-OOD performance degradation. **(Right) Snowball effect.** In temporal tracking, vanilla SAM2 [22] exhibits a snowball effect, with errors accumulating and causing irreversible performance drops. In contrast, our FreeVPS (orange line) maintains stable predictions over time, with highest temporal consistency score (TC = 0.747).

temporally consistent masks. Importantly, in the *detecting stage*, well-established foundations in the IPS community can be leveraged to obtain reliable predictions, either by utilizing off-the-shelf models or training a new model from scratch on various image datasets. The second *tracking stage*, operating independently to strengthen spatiotemporal coherence of masks from stage one, can also function as a post-processor to refine existing models’ predictions. However, considering current constraints on data scarcity, adopting the general-purpose track-by-detect models for VPS is non-trivial. Most methods [14–16] rely heavily on extensive video data for robust representation, while this data-hungry behavior is costly and impractical in the medical field. Other modular methods [17–19] integrate non-learning techniques (*e.g.*, Kalman filter [20]) and pre-trained models (*e.g.*, re-identification [21]) for spatiotemporal association. However, they exhibit limited adaptability in colonoscopy scenarios, where the Kalman filter’s linear assumption is incompatible with non-linear ego-motion of the colonoscope, and pre-trained re-identification models struggle to interpret medical visual patterns. Recall that the *detection stage* operates independently of the IPS model, allowing us to concentrate on optimizing the *tracking stage* in this study.

Recently, SAM2 [22] has achieved significant success in segmenting objects in videos, demonstrating robust tracking and generalization capabilities across general [23] and medical [24] scenarios. However, as shown in the right part of Fig. 1, its chain-rule memory mechanism suffers from **snowballing errors** in colonoscopy videos, leading to cumulative performance degradation over time. To alleviate such a snowball effect in the *tracking stage*, we repurpose SAM2 as a zero-shot video polyp segmenter, named FreeVPS, which consists of two consecutive steps. First, intra-association filtering (IAF) spatially aligns IPS’s multiframe output to a unified reference frame within a time window. It then establishes intra-associations among these aligned results, effectively filtering out inconsistencies while preserving consistent predictions. Second, inter-association refinement (IAR) constructs inter-associations between IAF-prompted masks and SAM-propagated masks from the preceding time window. This step adaptively identifies the appearance and disappearance of polyp instances and refines the segmentation of consistent polyp instances across frames. Our method synergistically integrates the IPS model with SAM2 in a training-free manner, achieving an improved balance between spatiotemporal modeling and domain generalization. The experiments show that FreeVPS outperforms existing IPS and VPS methods on both ID and OOD VPS datasets. These findings highlight the clinical potential of FreeVPS for real-world colonoscopy analysis.

In summary, our main contributions are as follows. **(a)** To the best of our knowledge, we are the first to recast the VPS task into a *track-by-detect* paradigm to allow each stage to specialize in distinct but synergistic sub-objectives. This paradigm effectively balances domain generalization in the *detecting stage* and spatiotemporal modeling in the *tracking stage*. **(b)** To alleviate the snowball effect of SAM2 in the *tracking stage*, we repurpose it as a zero-shot video polyp segmenter that comprises two consecutive modules. The intra-association filtering (IAF) eliminates spatial inaccuracies originating from the *detecting stage*, while the inter-association refinement (IAR) adaptively updates the memory bank to prevent error propagation over time. **(c)** Our FreeVPS achieves cutting-edge performance

on in-domain and out-of-domain generalizability, surpassing existing IPS and VPS paradigms. In a training-free manner, FreeVPS can boost the IPS model’s ID performance by 7.5% on SUN-SEG and OOD performance by 13.2% and 15.4% on PICCOLO and PolypGen, respectively. Importantly, on the untrimmed in-house video dataset, FreeVPS similarly significantly outperforms other methods.

2 Related Works

Image/Video Polyp Segmentation. With the advancement of deep learning, significant progress has been made in polyp segmentation, which can be primarily categorized into image- and video-based approaches. For image-based methods, seminal architectures like U-Net [25] and PraNet [5] have established the technical foundation. U-Net’s encoder-decoder structure enables effective multi-scale feature fusion, while PraNet pioneered coarse-to-fine boundary refinement, excelling at segmenting ambiguous polyp boundaries. Building upon these foundations, some methods have been further developed, such as introducing novel model architectures [26, 27], and unifying detection and segmentation [8]. These methods are supported by diverse and comprehensive polyp image datasets [28–33], which capture varied polyp types and imaging modalities, enabling models to learn robust contextual representations. However, image-based frameworks inherently lack the ability to leverage temporal information, limiting their applicability to colonoscopy videos. In contrast, video-based methods aim to exploit temporal dynamics for improved segmentation. Early works employed recurrent neural networks [34] or attention mechanisms [35, 9, 36] to fuse multi-frame features within fixed time windows. The latest development, SALI [12], introduced memory banks to aggregate long-term temporal cues, achieving SOTA performance. Despite architectural progress, VPS remains constrained by data diversity and scale. For instance, the largest VPS dataset, SUN-SEG [9], contains only about 100 distinct polyps across thousands of frames, reflecting the high cost of per-frame pixel-level annotation. Data scarcity limits video models’ application to real-world clinical scenarios, where polyp appearance and motion vary significantly.

Universal Temporal Propagation. In general scenarios, this category of methods is commonly referred to as semi-supervised video object segmentation, which propagates the initial ground truth (GT) segmentation of the first frame to the remaining entire video frames. Perhaps most notably among the many solutions, [37] innovatively introduced an external memory to explicitly store previously computed segmentation information, allowing the comprehensive use of past long-term segmentation cues. Based on this, many of the later excellent models [38–42], as well as the latest SAM2 [22], have adopted memory-based architectures. Using the largest video dataset SA-V, SAM2 shows strong zero-shot generalization capabilities, enabling it to segment various videos. To further enhance the temporal stability of SAM2, some methods [43–45] optimized for memory storage and deletion, but have not focused on snowballing errors. In contrast, our FreeVPS implements a synergistic *track-by-detect* framework specially designed for the colonoscopy domain, where human-annotated videos are expensive and scarce. Specifically, a polyp image segmenter with specific semantic knowledge continuously guides SAM2, effectively suppressing error accumulation in the memory bank. Another important difference is that we adapt SAM2 to be an automatic object-specific video segmenter, whereas all of the above methods require human intervention.

3 Methodology

As in §3.1, we first outline preliminaries of the introduced *track-by-detect* paradigm – IPS model for the *detecting* stage and SAM2 for the *tracking* stage – which form the basis for our FreeVPS. Next, we introduce two key modules to construct FreeVPS: intra-association filtering (IAF in §3.2) and inter-association refinement (IAR in §3.3).

3.1 Preliminaries

IPS model. This is used to obtain per-frame predictions during the *detecting* stage, and it can be any well-trained model. We denote its predictions as $\mathbf{M} = \{m_i\}_{i=1}^{|\mathbf{M}|}$, where each element m_i is a binary map indicating a single polyp instance, referred to as a *segment*. Notably, the different segments are non-overlapping: $m_i \cap m_j = \mathbf{0} (i \neq j)$, and $\mathbf{M} = \{\mathbf{0}\}$ when no polyp is detected in the image.

SAM2. We mainly let SAM2 perform its memory-based video tracking mechanism in the framework. Specifically, with video processing, several historical image-mask pairs $\{\mathcal{I}_{mem}, \mathcal{M}_{mem}\}$ are stored

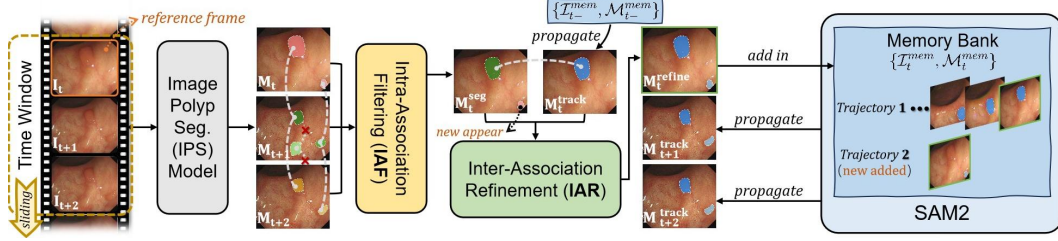


Figure 2: Overview of FreeVPS. We adopt an $N (= 3)$ -length non-overlapping sliding window. Within each window, we first employ the Intra-Association Filtering (IAF) to discover temporally consistent predictions of the image polyp segmentation (IPS) model over multiple frames. Then, we establish the Inter-Association Refinement (IAR) module to refine the propagation results of SAM2 through consistent predictions of the IPS model. The refined results are finally added in the memory bank of SAM2, driving it to temporal-consistently segment the remaining frames in the window.

in the memory bank. Given a query frame \mathbf{I}_q , SAM2 segments it by *propagating* the stored masks based on the calculated *correlation* between the stored images and the query frame:

$$\mathbf{M}_q^{track} = \{m_{q,n}^{track}\}_{n=1}^N = \text{Prop}(\mathcal{M}_{mem}, \text{Cor}(\mathcal{I}_{mem}, \mathbf{I}_q)), \quad (1)$$

where $\text{Prop}(\cdot, \cdot)$ and $\text{Cor}(\cdot, \cdot)$ represent the function of propagation and correlation in SAM2, respectively, N indicates the total number of object trajectories stored in the memory bank, and $m_{q,n}^{track}$ denotes the tracking result corresponding to the n -th object. Technically, SAM2 requires user-intervention and cannot actively discover new objects. To this end, we merge the ability of the IPS model to actively segment polyps and the long-term spatial-temporal consistency of SAM2 in a framework, realizing a robust automatic VPS model.

3.2 Intra-Association Filtering for Consistency Discovery of the IPS Model

The rapid camera movements and unstable lighting conditions in endoscopic videos result in numerous discrete low-quality frames, and IPS models are prone to discrete false predictions due to their inability to exploit multi-frame features. To generate more stable and reliable guidance from the IPS model for SAM2, we propose the IAF module.

Cross-Frame Alignment. As shown in Fig. 2, given video frames $\{\mathbf{I}_i\}_{i=t}^{t+T-1}$ withing a time window, where t and T denote the index of the first frame and the size of the window, respectively, the IAF module receives the corresponding segmentation result $\{\mathbf{M}_i\}_{i=t}^{t+T-1}$ generated by the IPS model. To prevent frame variations from interfering with the subsequent spatial-coincidence-based association, the segmentation results of all frames should be aligned to a unified frame, called *reference frame*. Subsequently, we define the first frame \mathbf{I}_t in each time window as the reference frame and align the segmentation results of the remaining frames with it. Considering that SAM2 is inherently well-suited for cross-image alignment, we utilize it to align the masks of all non-reference frame to the reference frame. Specifically, we store the image-mask pair of each frame in turn in the memory bank and set the reference frame as the query frame to obtain the aligned mask of each frame:

$$\overline{\mathbf{M}}_i = \text{Prop}(\mathbf{M}_i, \text{Cor}(\mathbf{I}_i, \mathbf{I}_t)), t+1 \leq i \leq t+T-1, \quad (2)$$

where $\overline{\mathbf{M}}_i$ is the spatially warped mask of \mathbf{M}_i aligned to the reference frame.

Tracklet Construction. To establish coherent mask tracklets, which record individual polyp instances consistently segmented by the IPS model across video frames, we propose a spatial coherence association mechanism. Initially, we merge the reference frame’s segmentation mask \mathbf{M}_t with the aligned masks $\{\overline{\mathbf{M}}_i\}_{i=t+1}^{t+T-1}$ of the remaining frames, followed by sorting all segments to yield a new segment set:

$$\mathcal{S} = \{s_k\} = \text{Sort}(\mathbf{M}_t \cup (\cup_{i=t+1}^{t+T-1} \overline{\mathbf{M}}_i)), \quad (3)$$

where $\text{Sort}(\cdot)$ primarily orders segments by decreasing temporal proximity to the reference frame, and secondarily by decreasing area size. Then, we compute a pairwise Intersection over Union (IoU) matrix $\mathbf{A} = [a_{ij}]_{|S| \times |S|}$, where the element a_{ij} quantifies the IoU between segments s_i and s_j . By defining that s_i and s_j are successfully paired if a_{ij} exceeds a predefined threshold θ , we

sequentially process the segments following their sorting priority in \mathcal{S} . For each candidate segment s_i , if it is paired successfully with remaining $T - 1$ segments from distinct frames, we create a set including this segment and its paired segments, called *tracklet*. Note that this formulation enforces the constraint that *one segment is forbidden to be repeatedly included in more than one tracklet*. In this way, assuming that we derive P tracklets, denoted as $\{tr_p\}_{p=1}^P$ and each tracklet $tr_p = \{s_k\}_{k \in \mathcal{K}_p}$, where \mathcal{K}_p represents the index set of all segments belonging to the p -th tracklet in \mathcal{S} .

Voting Filter. For each tracklet, we introduce a voting scheme to select the optimal segment that has the maximum sum of IoU scores with the rest segments in the tracklet, which is formulated as:

$$k_p^* = \arg \max_{k \in \mathcal{K}_p} \sum_{l \in \mathcal{K}_p, l \neq k} a_{kl}, \quad (4)$$

where k_p^* indicates the index of the representative segment in the p -th tracklet. We retain only these voted segments $\{s_{k_p^*}\}_{p=1}^P$ and serve them as the final output of the IAF module on the reference frame \mathbf{I}_t . For clarity, we denote the result as $\mathbf{M}_t^{seg} = \{m_{t,p}^{seg}\}_{p=1}^P$.

3.3 Inter-Association Refinement for Enhancing SAM2

To empower SAM2 with the capability of dynamically detecting new polyp instances while mitigating the snowballing errors, we introduce the IAR module, converting SAM2 into a fully automatic video segmenter through IAF-guided operation.

Inter-Association. Building upon the memory information preserved from the previous time window, denoted as \mathcal{I}_{t-}^{mem} , we let SAM2 track the reference frame of the current time window. Assuming that \mathcal{M}_{mem}^- stores Q object trajectories, the process yields the tracking result $\mathbf{M}_t^{track} = \{m_{t,q}^{track}\}_{q=1}^Q$. Next, we perform the Hungarian algorithm to associate \mathbf{M}_t^{track} and \mathbf{M}_t^{seg} . Inspired by [46], we pad the segment set with the smaller size using \emptyset (zero map), ensuring the equal size ($N = \max(P, Q)$) for both sets. Then we define the matching cost as IoU between segments and let the Hungarian algorithm [47] search for the optimal assignment of N elements $\sigma \in \mathfrak{S}_N$ with the lowest cost:

$$\hat{\sigma} = \arg \min_{\sigma \in \mathfrak{S}_N} \sum_q^N - \text{IoU}(m_{t,q}^{track}, m_{t,\sigma(q)}^{seg}). \quad (5)$$

Memory Refinement. To address the snowballing errors and perceive polyp appearance/disappearance in SAM2 tracking, we refine the memory by integrating \mathbf{M}_t^{track} and \mathbf{M}_t^{seg} according to the association result $\hat{\sigma}$. The refinement is based on an operation, denoted as $\mathcal{O}(\cdot, \cdot | \hat{\sigma})$, which is conditionally defined as follows. **(a)** For the matched two segments, *i.e.*, $m_{t,q}^{track}$ and $m_{t,\hat{\sigma}(q)}^{seg}$, we directly take their pixel-wise union $m_{t,q}^{track} \cup m_{t,\hat{\sigma}(q)}^{seg}$ as the final refined result on the reference frame of the polyp instance corresponding to the q -th trajectory stored in the memory. **(b)** For $m_{t,q}^{seg}$ matching with \emptyset , we consider it likely to be a newly appeared polyp instance founded by the IPS model. Furthermore, if the polyp appears in λ_1 consecutive time windows, we will keep $m_{t,q}^{seg}$ in the final refined result. **(c)** For $m_{t,p}^{track}$ matching with \emptyset , we consider that its corresponding polyp instance stored in the memory bank probably disappears. If it disappears in λ_2 consecutive time windows, the trajectory corresponding to the polyp instance will be removed from the memory. The final integrated result $\mathbf{M}_t^{refine} = \mathcal{O}(\mathbf{M}_t^{track}, \mathbf{M}_t^{seg} | \hat{\sigma})$ is regarded as the final segmentation result of the reference frame and added in the memory bank (as illustrated in Fig. 2). In particular, newly detected polyp instances are assigned unique identities in memory. The updated memory bank, denoted as $\{\mathcal{I}_t^{mem}, \mathcal{M}_t^{mem}\}$, is utilized to track the remaining frames in the current time window using Eq. (1), obtaining $\{\mathbf{M}_i^{track}\}_{i=t+1}^{t+T-1}$.

4 Experiments

4.1 Experimental Protocols

Datasets. We adopt the widely-used VPS dataset, SUN-SEG [9], as the ID data source. Its training set, referred to as \mathcal{D}_V , comprises 112 video clips totaling 19,544 frames, and its testing set contains 173 video clips totaling 29,592 frames. To quantify generalizability in OOD scenarios, we also

Table 1: Comparisons on an ID dataset (SUN-SEG [9]) and two OOD datasets (PICCOLO [48], PolypGen [49]). “†” indicates that SAM2 is fully fine-tuned on video data \mathcal{D}_V with official code.

Models	Train Data	SUN-SEG (§4.2)				PICCOLO (§4.3)				PolypGen (§4.3)			
		Dice	IoU	MAE	TC	Dice	IoU	MAE	TC	Dice	IoU	MAE	TC
► <i>Image Polyp Segmentation Models</i>													
PolypPVT [26]	\mathcal{D}_V	78.6	70.6	4.0	69.4	51.9	42.7	14.7	64.2	35.5	28.2	12.3	60.0
Polyper [50]	\mathcal{D}_V	79.7	71.1	3.7	69.8	54.4	43.3	13.8	64.2	38.3	32.7	10.5	61.2
QueryNet [8]	\mathcal{D}_V	80.5	72.1	3.4	70.1	58.9	51.3	10.5	64.5	41.2	34.3	10.3	61.0
QueryNet [8]	$\mathcal{D}_V + \mathcal{D}_I$	82.2	73.8	2.8	70.5	68.0	62.2	7.7	66.2	53.2	46.7	4.7	63.4
► <i>Video Polyp Segmentation Models</i>													
PNS+ [9]	\mathcal{D}_V	80.9	73.3	3.4	73.3	53.1	44.9	14.2	67.8	44.1	37.5	8.1	64.2
AEN [36]	\mathcal{D}_V	81.9	72.4	3.4	72.9	58.2	50.5	11.3	67.6	44.8	38.1	8.1	63.9
Diff-VPS [10]	\mathcal{D}_V	82.7	75.3	2.9	72.8	63.4	55.0	8.2	67.8	44.3	37.2	8.4	64.3
Vivim [11]	\mathcal{D}_V	83.2	74.4	3.0	73.2	66.2	58.5	8.3	68.1	48.4	42.4	6.6	64.3
SALI [12]	\mathcal{D}_V	86.6	80.0	2.3	73.7	69.7	62.7	6.9	68.4	50.8	45.0	5.1	64.5
► <i>Image segmentor: QueryNet</i>													
+ FreeVPS	\mathcal{D}_V	87.5	80.3	2.0	74.2	72.8	66.4	6.4	69.2	54.0	48.6	4.4	65.3
+ FreeVPS	$\mathcal{D}_V + \mathcal{D}_I$	88.4	82.5	1.6	74.7	77.0	71.5	6.0	70.0	61.4	54.3	3.3	65.8
+ FreeVPS [†]	$\mathcal{D}_V + \mathcal{D}_I$	90.2	84.8	1.3	75.1	83.1	77.4	5.5	70.2	65.3	59.1	2.8	66.2

include two public VPS datasets: PICCOLO [48] (39 video clips, 3, 433 frames) and PolypGen [49] (23 video clips, 8, 037 frames). However, these VPS benchmarks usually consist of human-trimmed videos, assuming each frame contains at least one polyp. This assumption restricts the model’s applicability to real-world clinical scenarios, where frames without polyps or other findings are common. To address this gap, we create an in-house dataset, LU-VPS, comprising nine positive and six negative long untrimmed colonoscopy videos from real clinical procedures. The video durations span 20~50 minutes at 15FPS. To guarantee reliability, three expert endoscopists with 15-20 years of clinical experience annotated our LU-VPS, yielding 59, 104 bounding boxes and 48, 282 masks for polyps. For more details like data statistics and visualizations, refer to the [APPENDIX](#). We introduce six public IPS datasets to fully leverage abundant image resources: ClinicDB [29], Kvasir-SEG [32], ColonDB [30], EndoScene [31], ETIS [28], and PS-NBI2K [33], totaling 5, 026 images. These images, termed \mathcal{D}_I , will be used exclusively to train the IPS model for robust spatial representation.

Evaluation Metrics. We mainly focus on verifying the performance of the model in semantic video segmentation and employ four metrics to evaluate VPS performance, including Dice, intersection over union (IoU), mean absolute error (MAE) and temporal consistency (TC) [51].

Implementation Details. Recall that FreeVPS functions as a training-free post-processor to refine temporal masks from any IPS model. In subsequent experiments, we used the cutting-edge model, QueryNet [8], as a representative example to build FreeVPS. More validations on other IPS models are provided in the [APPENDIX](#). FreeVPS is built upon SAM2 [22] with Hiera-B+ [52], using the PyTorch framework [53] and is inferred on a single NVIDIA GeForce RTX 4090 GPU with 24GB memory. Based on the ablation studies in §4.5, we set the length of time windows $T = 3$ and the paired threshold $\theta = 0.5$. Moreover, we empirically set $\{\lambda_1, \lambda_2\} = \{1, 3\}$ in memory management.

Baseline Models. As shown in Tab. 1, we select several of the latest polyp segmentation models, including three IPS models [26, 50, 8] and five VPS models [9, 36, 10–12]. Notably, current VPS models are all trained in the SUN-SEG training set \mathcal{D}_V . Therefore, we retrain three IPS models on the same set \mathcal{D}_V to ensure a fair comparison between image- and video-based models.

4.2 In-domain Performance

Tab. 1 reports the ID performance of advanced polyp segmentation models, *i.e.*, “SUN-SEG (train set) \Rightarrow SUN-SEG (test set)”. When trained on \mathcal{D}_V , FreeVPS outperforms its image-based counterpart, QueryNet, by 7.0% in Dice and 4.1% in TC. This improvement demonstrates that our method significantly improves the video segmentation performance based on existing IPS models. Furthermore, we outperform all other video-based models on the same training data, especially surpassing the runner-up, SALI [12], by 1.9% in Dice. To further explore potential performance improvements, we investigate two strategies. First, we retrain the IPS model, QueryNet, using the combined set of \mathcal{D}_V and \mathcal{D}_I . We observe that our FreeVPS with QueryNet ($\mathcal{D}_V + \mathcal{D}_I$) achieved an IoU increase from 80.3% to 82.5%, primarily due to enhanced spatial-context learning. Second, we unlock SAM2’s

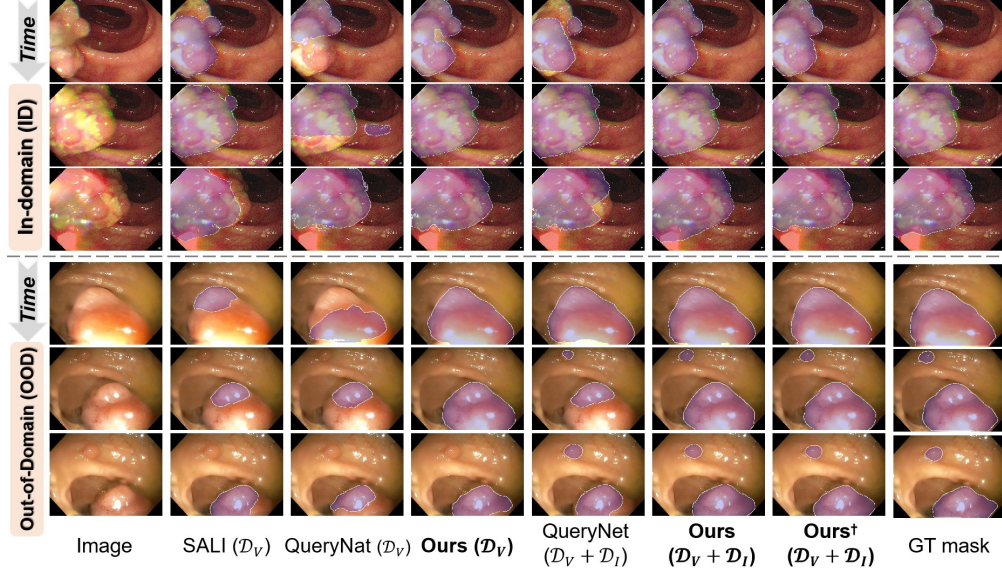


Figure 3: Prediction visualization on ID (SUN-SEG [9]) and OOD (PolypGen [49]) datasets.

spatiotemporal learning capacity by fully fine-tuning it on video data \mathcal{D}_V . Unless otherwise specified, FreeVPS in the following analysis is built on QueryNet (trained on $\mathcal{D}_I + \mathcal{D}_V$), while SAM2 operates in a training-free manner, as indicated in the second-last row of Tab. 1. In the upper part of Fig. 3, we qualitatively visualize the ID predictions of competing models in various settings. These visualizations demonstrate that FreeVPS effectively mitigates the discrete false-positive regions predicted by QueryNet, resulting in more accurate and temporally consistent segmentation results. Notably, when trained solely on \mathcal{D}_V , FreeVPS (fourth column) produces predictions that align more closely with ground-truth masks (last column) compared to the video model SALI (second column). Moreover, with the extra image data \mathcal{D}_I , the performance of QueryNet and FreeVPS is further refined.

4.3 Out-of-domain Generalization

Cross-domain generalization is a critical criterion for VPS models segmentation models in real clinical deployment. To assess the OOD generalizability of all competing methods, we adopt two unseen VPS dataset to form a “SUN-SEG (train set) \Rightarrow PICCOLO/PolypGen” evaluation pipeline. As reported in Tab. 1, when trained only on \mathcal{D}_V , FreeVPS outperforms other models on both unseen datasets, demonstrating robust cross-domain generalizability. With the inclusion of additional training data \mathcal{D}_I , both QueryNet and FreeVPS exhibit substantial improvements in OOD generalization. Specifically, QueryNet improves Dice by 9.1% and 12% on PICCOLO and PolypGen, respectively, while FreeVPS achieves further gains of 4.2% and 7.4% in Dice. This gain is primarily attributed to the diverse polyp appearances learned from \mathcal{D}_I , which provide richer contextual knowledge for representation. As shown in the lower part of Fig. 3, training on the combined datasets (*i.e.*, $\mathcal{D}_V + \mathcal{D}_I$) enables the model to identify previously missed, small-sized occult polyps, highlighting the benefits of enriched spatiotemporal learning. These results underscore the effectiveness of repurposing a robust video foundation model with our core innovations for enhanced ID-to-OOD generalization.

4.4 Out-of-domain Generalization on Long-Untrimmed Colonoscopy Videos

Existing public VPS datasets usually presume that each frame contains at least one polyp, thus trimming videos into short clips of up to tens of seconds during data processing. However, in real clinical practice, raw colonoscopic videos often span tens of minutes, presenting more complex and challenging scenarios. To evaluate the long-term tracking capacity of competing models in clinical scenarios, we use an in-house dataset, LU-VPS, to assess both temporal detection and segmentation performance over long-untrimmed videos. Specifically, we calculate the detection metrics (*i.e.*, $F1_{50}$, AP_{50} , $AP_{50:95}$) based on all frames and test the segmentation metrics (*i.e.*, Dice, IoU) only on positive polyps. We include three categories of models for comparison: object detection methods [54–56], semantic segmentation methods [50, 11, 12], and unified detection and segmentation methods [57, 8].

Table 2: Comparisons on the in-house dataset (LU-VPS). For segmentation models, the detection performance is evaluated by converting their output masks into the corresponding tightest bounding boxes. “n/a” denotes that the evaluation metric is not applicable.

Models	Model type	Train data	Label type	@Detection			@Segmentation	
				F1 ₅₀	AP ₅₀	AP _{50:95}	Dice	IoU
YOLOv11 [54]	Image	$\mathcal{D}_I + \mathcal{D}_V$	Box	40.7	37.1	25.0	n/a	n/a
Relation-DETR [55]	Image	$\mathcal{D}_I + \mathcal{D}_V$	Box	44.0	39.1	26.7	n/a	n/a
TSdetector [56]	Video	\mathcal{D}_V	Box	43.5	42.2	27.3	n/a	n/a
Polyper [50]	Image	$\mathcal{D}_I + \mathcal{D}_V$	Mask	18.3	n/a	n/a	58.7	51.1
Vivim [11]	Video	\mathcal{D}_V	Mask	14.6	n/a	n/a	51.6	43.5
SALI [12]	Video	\mathcal{D}_V	Mask	19.1	n/a	n/a	55.0	47.8
Mask2Former [57]	Image	$\mathcal{D}_I + \mathcal{D}_V$	Box+Mask	50.3	47.7	30.6	61.8	56.9
QueryNet [8]	Image	$\mathcal{D}_I + \mathcal{D}_V$	Box+Mask	51.5	45.6	29.4	63.7	57.0
FreeVPS (Ours)	Video	$\mathcal{D}_I + \mathcal{D}_V$	Box+Mask	63.0	52.4	33.8	68.2	62.8

As shown in Tab. 2, semantic segmentation models generally exhibit poorer detection performance compared to the other two types of models, which is attributed to their lack of architectural design and training objectives specifically for the detection task. In contrast, FreeVPS achieves the highest performance in both detection and segmentation tasks in long-untrimmed colonoscopy videos. This success underscores its potential for open-set clinical scenarios.

4.5 Diagnostic Experiments

Effectiveness of Key Components.

To validate the effectiveness of two key components of FreeVPS, the IAF and IAR modules, we test two variants of FreeVPS by disabling IAF or IAR, the IPS baseline QueryNet on SUN-SEG. As shown in the lower part of Fig. 4, the model variant (#c) illustrates that removing the IAF module causes the noise predictions from the IPS model to propagate throughout the pipeline, ultimately degrading performance and even falling behind the baseline in Dice, IoU, and MAE metrics. Similarly, as in model (#b), removing the IAR module disrupts temporal modeling, affecting temporal consistency. More clearly in the upper part of Fig. 4, the variant (#c) retains the false positive prediction of the IPS model to be retained and be persistently segmented in the video stream. The temporal stability of the segmentation of the variant (#b) decreases, especially in the region of polyp boundaries. In summary, IAF and IAR are mutually beneficial and together play an important role in combining the IPS model and SAM2.

Effectiveness of the Sub-components in IAF.

We conduct experiments to assess the effectiveness of cross-frame alignment and voting filter proposed in the IAF module. For cross-frame alignment, we evaluate three settings: (1) disabling alignment and directly associating multiple IPS predictions, (2) applying an optical flow-based alignment method [51], and (3) our proposed SAM2-based alignment strategy. Furthermore, we compare our voting filter method with a variant that randomly selects a segment from each tracklet. As shown in Table 3, both our SAM2-based alignment and voting filter are superior. Although optical flow-based alignment shows slight improvement over the no-alignment setting, its effectiveness is limited due to the unstable lighting conditions in the colonoscopy environment. In contrast, our proposed alignment method leverages SAM2’s robust representations to achieve more consistent cross-frame associations, leading to substantial performance gains.

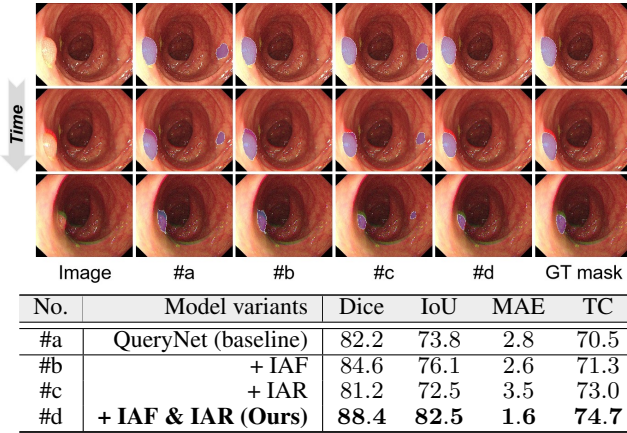


Figure 4: Ablation study on IAF and IAR modules: qualitative (upper) and quantitative results (lower).

Table 3: Ablation study on IAF module.

Model variants	Dice	IoU	MAE
w/o align.	84.1	75.5	2.5
Optical flow-based align. [51]	84.8	76.5	2.3
SAM2-based align. (Ours)	88.4	82.5	1.6
w/o Voting filter (random)	85.6	78.2	2.5
Voting filter (Ours)	88.4	82.5	1.6

Comparisons with Track-by-Detect Bridge Modules.

We compare our FreeVPS with four track-by-detect bridge modules that can adapt image models to the video domain, including two end-to-end methods [13, 14] and two modular methods [18, 19]. We uniformly set QueryNet as their image segmenters. For end-to-end methods, we perform a two-stage training strategy, first training the image segmenter independently on the union of \mathcal{D}_I and \mathcal{D}_V and second training its entire framework on \mathcal{D}_V , while for modular methods, we implement them by directly combining the well-trained image segmenter on the union of \mathcal{D}_I and \mathcal{D}_V with their bridge modules. Specially, we retrain a ReID model on polyp datasets for [19]. As shown in Tab. 4, modular methods typically outperform end-to-end methods in OOD generalization because the bridge modules of end-to-end methods are trained only on limited polyp video data with limited generalization. Compared to motion matching and appearance matching used by [18, 19], SAM2 implicitly learns more stable and unified spatio-temporal feature representations of objects from large-scale video data [22], which contributes to the superiority of our method.

Hyperparameters configuration. As in Tab. 5, we evaluate FreeVPS’s performance on SUN-SEG dataset with two hyperparameters: the length of time window T and the association threshold θ of IAF. With $T = 2$, the voting filter in Eq. (4) is ineffective, prompting us to select one of the two segments from the frames at random. We find that the best results occur with $T = 3$ and $\theta = 0.5$, which we use as our default configuration.

Versatility for General Scenarios.

FreeVPS is a plug-and-play framework that can be seamlessly integrated with any image segmentation model to enhance its performance in videos. We further validate FreeVPS versatility on general scenarios [13, 59] by adding it to two representative image segmenters [60, 61]. As reported in Tab. 6, FreeVPS enables both image segmenters to achieve superior performance on video instance segmentation. Notably, unlike competing methods (*i.e.*, MaskTrack [13], CrossVIS [16]) that require training from scratch on video data, we directly use training-free SAM2 to achieve better performance, making it more deployment-friendly.

5 Conclusion

In this work, we propose FreeVPS, which novelly implements the track-by-detect paradigm in VPS, effectively integrating the domain generalization of the IPS method with the spatiotemporal modeling of SAM2 in a training-free manner. To address SAM2’s inherent limitation of snowballing errors, we propose two key cascade modules, IAF and IAR. Within each time window, IAR establishes associations between the IAR-filtered IPS predictions and SAM2 to dynamically and continuously manage the SAM2’s memory bank, forming an automatic and efficient VPS framework. Extensive experiments show that FreeVPS achieves SOTA performance on ID and OOD datasets compared to the existing IPS and VPS methods. In addition, FreeVPS shows promising performance in the in-house untrimmed colonoscopy video dataset. These results highlight the potential of FreeVPS for real clinical applications. In future work, we plan to address the representation limitations of existing IPS models by developing a robust colonoscopy-specific foundation model. This will involve constructing a large-scale, diverse polyp dataset to enhance IPS capabilities and further strengthen the effectiveness of our FreeVPS.

Table 4: Comparisons with other track-by-detect bridge methods on ID and OOD scenarios.

Methods		SUN-SEG		LU-VPS	
		Dice	TC	Dice	TC
End-to-End	MaskTrack [13]	82.8	72.4	50.4	64.1
	CTVIS [58]	85.7	73.5	58.1	64.5
Modular	DEVA [18]	79.8	72.0	62.6	64.5
	StrongSORT [19]	83.0	72.3	64.3	64.8
	FreeVPS (Ours)	88.4	74.7	68.2	65.7

Table 5: Ablation study on hyperparameters T and θ .

T	Dice	IoU	MAE	θ	Dice	IoU	MAE
2	86.9	80.8	2.0	0.3	87.4	81.7	2.0
3	88.4	82.5	1.6	0.4	88.0	81.9	1.8
4	87.8	81.5	1.8	0.5	88.4	82.5	1.6
5	87.0	80.3	2.2	0.6	88.1	82.1	1.6

Table 6: Versatility on YouTube-VIS 2019 [13] & 2021 [59].

Models	YouTube-VIS-2019			YouTube-VIS-2021		
	AP	AP ₅₀	AR ₁	AP	AP ₅₀	AR ₁
► <i>Image Segmenter: Mask R-CNN</i> [60]						
+ MaskTrack [13]	30.3	51.1	31.0	28.6	48.9	26.5
+ FreeVPS (Ours)	42.3	66.0	41.9	40.2	62.0	35.3
► <i>Image Segmenter: CondInst</i> [61]						
+ CrossVIS [16]	34.8	54.6	34.0	33.3	53.8	30.1
+ FreeVPS (Ours)	43.8	66.3	42.7	41.7	62.7	37.2

References

- [1] Aasma Shaukat and Theodore R Levin. Current and future colorectal cancer screening strategies. *Nature reviews Gastroenterology & hepatology*, 19(8):521–531, 2022.
- [2] Hermann Brenner, Thomas Heisser, Rafael Cardoso, and Michael Hoffmeister. Reduction in colorectal cancer incidence by screening endoscopy. *Nature Reviews Gastroenterology & Hepatology*, 21(2):125–133, 2024.
- [3] Ge-Peng Ji, Jingyi Liu, Peng Xu, Nick Barnes, Fahad Shahbaz Khan, Salman Khan, and Deng-Ping Fan. Frontiers in intelligent colonoscopy. *arXiv preprint arXiv:2410.17241*, 2024.
- [4] Yuqi Fang, Cheng Chen, Yixuan Yuan, and Kai-yu Tong. Selective feature aggregation network with area-boundary constraints for polyp segmentation. In *Medical Image Computing and Computer Assisted Intervention–MICCAI 2019: 22nd International Conference, Shenzhen, China, October 13–17, 2019, Proceedings, Part I 22*, pages 302–310. Springer, 2019.
- [5] Deng-Ping Fan, Ge-Peng Ji, Tao Zhou, Geng Chen, Huazhu Fu, Jianbing Shen, and Ling Shao. Pranet: Parallel reverse attention network for polyp segmentation. In *International conference on medical image computing and computer-assisted intervention*, pages 263–273. Springer, 2020.
- [6] Xiaoqing Guo, Zhen Chen, Jun Liu, and Yixuan Yuan. Non-equivalent images and pixels: Confidence-aware resampling with meta-learning mixup for polyp segmentation. *Medical image analysis*, 78:102394, 2022.
- [7] Yuxuan Shi, Hong Wang, Haoqin Ji, Haozhe Liu, Yuexiang Li, Nanjun He, Dong Wei, Yawen Huang, Qi Dai, Jianrong Wu, et al. A deep weakly semi-supervised framework for endoscopic lesion segmentation. *Medical Image Analysis*, 90:102973, 2023.
- [8] Jiaxing Chai, Zhiming Luo, Jianzhe Gao, Licun Dai, Yingxin Lai, and Shaozi Li. Querynet: A unified framework for accurate polyp segmentation and detection. In *International Conference on Medical Image Computing and Computer-Assisted Intervention*, pages 544–554. Springer, 2024.
- [9] Ge-Peng Ji, Guobao Xiao, Yu-Cheng Chou, Deng-Ping Fan, Kai Zhao, Geng Chen, and Luc Van Gool. Video polyp segmentation: A deep learning perspective. *Machine Intelligence Research*, 19(6):531–549, 2022.
- [10] Yingling Lu, Yijun Yang, Zhaohu Xing, Qiong Wang, and Lei Zhu. Diff-vps: Video polyp segmentation via a multi-task diffusion network with adversarial temporal reasoning. In *International Conference on Medical Image Computing and Computer-Assisted Intervention*, pages 165–175. Springer, 2024.
- [11] Yijun Yang, Zhaohu Xing, Lequan Yu, Chunwang Huang, Huazhu Fu, and Lei Zhu. Vivim: A video vision mamba for medical video segmentation. *arXiv preprint arXiv:2401.14168*, 2024.
- [12] Qiang Hu, Zhenyu Yi, Ying Zhou, Fang Peng, Mei Liu, Qiang Li, and Zhiwei Wang. Sali: Short-term alignment and long-term interaction network for colonoscopy video polyp segmentation. In *International Conference on Medical Image Computing and Computer-Assisted Intervention*, pages 531–541. Springer, 2024.
- [13] Linjie Yang, Yuchen Fan, and Ning Xu. Video instance segmentation. In *Proceedings of the IEEE/CVF international conference on computer vision*, pages 5188–5197, 2019.
- [14] Jiale Cao, Rao Muhammad Anwer, Hisham Cholakkal, Fahad Shahbaz Khan, Yanwei Pang, and Ling Shao. Sipmask: Spatial information preservation for fast image and video instance segmentation. In *Computer Vision–ECCV 2020: 16th European Conference, Glasgow, UK, August 23–28, 2020, Proceedings, Part XIV 16*, pages 1–18. Springer, 2020.
- [15] Dongfang Liu, Yiming Cui, Wenbo Tan, and Yingjie Chen. Sg-net: Spatial granularity network for one-stage video instance segmentation. In *Proceedings of the IEEE/CVF conference on computer vision and pattern recognition*, pages 9816–9825, 2021.

- [16] Shusheng Yang, Yuxin Fang, Xinggang Wang, Yu Li, Chen Fang, Ying Shan, Bin Feng, and Wenyu Liu. Crossover learning for fast online video instance segmentation. In *proceedings of the IEEE/CVF international conference on computer vision*, pages 8043–8052, 2021.
- [17] Balaji Veeramani, John W Raymond, and Pritam Chanda. Deepsort: deep convolutional networks for sorting haploid maize seeds. *BMC bioinformatics*, 19:1–9, 2018.
- [18] Ho Kei Cheng, Seoung Wug Oh, Brian Price, Alexander Schwing, and Joon-Young Lee. Tracking anything with decoupled video segmentation. In *Proceedings of the IEEE/CVF International Conference on Computer Vision*, pages 1316–1326, 2023.
- [19] Yunhao Du, Zhicheng Zhao, Yang Song, Yanyun Zhao, Fei Su, Tao Gong, and Hongying Meng. Strongsort: Make deepsort great again. *IEEE Transactions on Multimedia*, 25:8725–8737, 2023.
- [20] Rudolph Emil Kalman. A new approach to linear filtering and prediction problems. 1960.
- [21] Hao Luo, Wei Jiang, Youzhi Gu, Fuxu Liu, Xingyu Liao, Shenqi Lai, and Jianyang Gu. A strong baseline and batch normalization neck for deep person re-identification. *IEEE Transactions on Multimedia*, 22(10):2597–2609, 2019.
- [22] Nikhila Ravi, Valentin Gabeur, Yuan-Ting Hu, Ronghang Hu, Chaitanya Ryali, Tengyu Ma, Haitham Khedr, Roman Rädle, Chloe Rolland, Laura Gustafson, et al. Sam 2: Segment anything in images and videos. *arXiv preprint arXiv:2408.00714*, 2024.
- [23] Chunhui Zhang, Yawen Cui, Weilin Lin, Guanjie Huang, Yan Rong, Li Liu, and Shiguang Shan. Segment anything for videos: A systematic survey. *arXiv preprint arXiv:2408.08315*, 2024.
- [24] Jun Ma, Sumin Kim, Feifei Li, Mohammed Baharoon, Reza Asakereh, Hongwei Lyu, and Bo Wang. Segment anything in medical images and videos: Benchmark and deployment. *arXiv preprint arXiv:2408.03322*, 2024.
- [25] Olaf Ronneberger, Philipp Fischer, and Thomas Brox. U-net: Convolutional networks for biomedical image segmentation. In *Medical image computing and computer-assisted intervention–MICCAI 2015: 18th international conference, Munich, Germany, October 5-9, 2015, proceedings, part III 18*, pages 234–241. Springer, 2015.
- [26] Bo Dong, Wenhai Wang, Deng-Ping Fan, Jinpeng Li, Huazhu Fu, and Ling Shao. Polyp-pvt: Polyp segmentation with pyramid vision transformers. *arXiv preprint arXiv:2108.06932*, 2021.
- [27] Zhongxing Xu, Feilong Tang, Zhe Chen, Zheng Zhou, Weishan Wu, Yuyao Yang, Yu Liang, Jiyu Jiang, Xuyue Cai, and Jionglong Su. Polyp-mamba: Polyp segmentation with visual mamba. In *International Conference on Medical Image Computing and Computer-Assisted Intervention*, pages 510–521. Springer, 2024.
- [28] Juan Silva, Aymeric Histace, Olivier Romain, Xavier Dray, and Bertrand Granado. Toward embedded detection of polyps in wce images for early diagnosis of colorectal cancer. *International journal of computer assisted radiology and surgery*, 9:283–293, 2014.
- [29] Jorge Bernal, F Javier Sánchez, Gloria Fernández-Esparrach, Debora Gil, Cristina Rodríguez, and Fernando Vilariño. Wm-dova maps for accurate polyp highlighting in colonoscopy: Validation vs. saliency maps from physicians. *Computerized medical imaging and graphics*, 43:99–111, 2015.
- [30] Nima Tajbakhsh, Suryakanth R Gurudu, and Jianming Liang. Automated polyp detection in colonoscopy videos using shape and context information. *IEEE transactions on medical imaging*, 35(2):630–644, 2015.
- [31] David Vázquez, Jorge Bernal, F Javier Sánchez, Gloria Fernández-Esparrach, Antonio M López, Adriana Romero, Michal Drozdal, Aaron Courville, et al. A benchmark for endoluminal scene segmentation of colonoscopy images. *Journal of healthcare engineering*, 2017, 2017.

- [32] Debesh Jha, Pia H Smedsrud, Michael A Riegler, Pål Halvorsen, Thomas de Lange, Dag Johansen, and Håvard D Johansen. Kvasir-seg: A segmented polyp dataset. In *MultiMedia Modeling: 26th International Conference, MMM 2020, Daejeon, South Korea, January 5–8, 2020, Proceedings, Part II* 26, pages 451–462. Springer, 2020.
- [33] Guanghui Yue, Guibin Zhuo, Siying Li, Tianwei Zhou, Jingfeng Du, Weiqing Yan, Jingwen Hou, Weide Liu, and Tianfu Wang. Benchmarking polyp segmentation methods in narrow-band imaging colonoscopy images. *IEEE Journal of Biomedical and Health Informatics*, 27(7):3360–3371, 2023.
- [34] Juana González-Bueno Puyal, Kanwal K Bhatia, Patrick Brandao, Omer F Ahmad, Daniel Toth, Rawen Kader, Laurence Lovat, Peter Mountney, and Danail Stoyanov. Endoscopic polyp segmentation using a hybrid 2d/3d cnn. In *Medical Image Computing and Computer Assisted Intervention–MICCAI 2020: 23rd International Conference, Lima, Peru, October 4–8, 2020, Proceedings, Part VI* 23, pages 295–305. Springer, 2020.
- [35] Ge-Peng Ji, Yu-Cheng Chou, Deng-Ping Fan, Geng Chen, Huazhu Fu, Debesh Jha, and Ling Shao. Progressively normalized self-attention network for video polyp segmentation. In *International Conference on Medical Image Computing and Computer-Assisted Intervention*, pages 142–152. Springer, 2021.
- [36] Zhixue Fang, Xinrong Guo, Jingyin Lin, Huisi Wu, and Jing Qin. An embedding-unleashing video polyp segmentation framework via region linking and scale alignment. In *Proceedings of the AAAI conference on artificial intelligence*, volume 38, pages 1744–1752, 2024.
- [37] Seoung Wug Oh, Joon-Young Lee, Ning Xu, and Seon Joo Kim. Video object segmentation using space-time memory networks. In *Proceedings of the IEEE/CVF international conference on computer vision*, pages 9226–9235, 2019.
- [38] Goutam Bhat, Felix Järemo Lawin, Martin Danelljan, Andreas Robinson, Michael Felsberg, Luc Van Gool, and Radu Timofte. Learning what to learn for video object segmentation. In *Computer Vision–ECCV 2020: 16th European Conference, Glasgow, UK, August 23–28, 2020, Proceedings, Part II* 16, pages 777–794. Springer, 2020.
- [39] Andreas Robinson, Felix Jaremo Lawin, Martin Danelljan, Fahad Shahbaz Khan, and Michael Felsberg. Learning fast and robust target models for video object segmentation. In *Proceedings of the IEEE/CVF conference on computer vision and pattern recognition*, pages 7406–7415, 2020.
- [40] Ho Kei Cheng, Yu-Wing Tai, and Chi-Keung Tang. Rethinking space-time networks with improved memory coverage for efficient video object segmentation. *Advances in Neural Information Processing Systems*, 34:11781–11794, 2021.
- [41] Hongje Seong, Junhyuk Hyun, and Euntai Kim. Video object segmentation using kernelized memory network with multiple kernels. *IEEE transactions on pattern analysis and machine intelligence*, 45(2):2595–2612, 2022.
- [42] Yurong Zhang, Liulei Li, Wenguan Wang, Rong Xie, Li Song, and Wenjun Zhang. Boosting video object segmentation via space-time correspondence learning. In *Proceedings of the IEEE/CVF Conference on Computer Vision and Pattern Recognition*, pages 2246–2256, 2023.
- [43] Cheng-Yen Yang, Hsiang-Wei Huang, Wenhao Chai, Zhongyu Jiang, and Jenq-Neng Hwang. Samurai: Adapting segment anything model for zero-shot visual tracking with motion-aware memory. *arXiv preprint arXiv:2411.11922*, 2024.
- [44] Shuangrui Ding, Rui Qian, Xiaoyi Dong, Pan Zhang, Yuhang Zang, Yuhang Cao, Yuwei Guo, Dahua Lin, and Jiaqi Wang. Sam2long: Enhancing sam 2 for long video segmentation with a training-free memory tree. *arXiv preprint arXiv:2410.16268*, 2024.
- [45] Jovana Videnovic, Alan Lukezic, and Matej Kristan. A distractor-aware memory for visual object tracking with sam2. *arXiv preprint arXiv:2411.17576*, 2024.

- [46] Nicolas Carion, Francisco Massa, Gabriel Synnaeve, Nicolas Usunier, Alexander Kirillov, and Sergey Zagoruyko. End-to-end object detection with transformers. In *European conference on computer vision*, pages 213–229. Springer, 2020.
- [47] Harold W Kuhn. The hungarian method for the assignment problem. *Naval research logistics quarterly*, 2(1-2):83–97, 1955.
- [48] Luisa F Sánchez-Peralta, J Blas Pagador, Artzai Picón, Ángel José Calderón, Francisco Polo, Nagore Andracka, Roberto Bilbao, Ben Glover, Cristina L Saratxaga, and Francisco M Sánchez-Margallo. Piccolo white-light and narrow-band imaging colonoscopic dataset: A performance comparative of models and datasets. *Applied Sciences*, 10(23):8501, 2020.
- [49] Sharib Ali, Debesh Jha, Noha Ghatwary, Stefano Realdon, Renato Cannizzaro, Osama E Salem, Dominique Lamarque, Christian Daul, Michael A Riegler, Kim V Anonsen, et al. A multi-centre polyp detection and segmentation dataset for generalisability assessment. *Scientific Data*, 10(1):75, 2023.
- [50] Hao Shao, Yang Zhang, and Qibin Hou. Polyper: Boundary sensitive polyp segmentation. In *Proceedings of the AAAI Conference on Artificial Intelligence*, volume 38, pages 4731–4739, 2024.
- [51] Yifan Liu, Chunhua Shen, Changqian Yu, and Jingdong Wang. Efficient semantic video segmentation with per-frame inference. In *Computer Vision–ECCV 2020: 16th European Conference, Glasgow, UK, August 23–28, 2020, Proceedings, Part X 16*, pages 352–368. Springer, 2020.
- [52] Chaitanya Ryali, Yuan-Ting Hu, Daniel Bolya, Chen Wei, Haoqi Fan, Po-Yao Huang, Vaibhav Aggarwal, Arkabandhu Chowdhury, Omid Poursaeed, Judy Hoffman, et al. Hiera: A hierarchical vision transformer without the bells-and-whistles. In *International Conference on Machine Learning*, pages 29441–29454. PMLR, 2023.
- [53] Adam Paszke, Sam Gross, Francisco Massa, Adam Lerer, James Bradbury, Gregory Chanan, Trevor Killeen, Zeming Lin, Natalia Gimelshein, Luca Antiga, et al. Pytorch: An imperative style, high-performance deep learning library. *Advances in neural information processing systems*, 32, 2019.
- [54] Glenn Jocher and Jing Qiu. Ultralytics yolo11, 2024.
- [55] Xiuquan Hou, Meiqin Liu, Senlin Zhang, Ping Wei, Badong Chen, and Xuguang Lan. Relation detr: Exploring explicit position relation prior for object detection. In *European Conference on Computer Vision*, pages 89–105. Springer, 2024.
- [56] Kai-Ni Wang, Haolin Wang, Guang-Quan Zhou, Yangang Wang, Ling Yang, Yang Chen, and Shuo Li. Tsdetector: Temporal–spatial self-correction collaborative learning for colonoscopy video detection. *Medical Image Analysis*, 100:103384, 2025.
- [57] Bowen Cheng, Ishan Misra, Alexander G Schwing, Alexander Kirillov, and Rohit Girdhar. Masked-attention mask transformer for universal image segmentation. In *Proceedings of the IEEE/CVF conference on computer vision and pattern recognition*, pages 1290–1299, 2022.
- [58] Kaining Ying, Qing Zhong, Weian Mao, Zhenhua Wang, Hao Chen, Lin Yuanbo Wu, Yifan Liu, Chengxiang Fan, Yunzhi Zhuge, and Chunhua Shen. Ctvis: Consistent training for online video instance segmentation. In *Proceedings of the IEEE/CVF International Conference on Computer Vision*, pages 899–908, 2023.
- [59] Ning Xu, Linjie Yang, Jianchao Yang, Dingcheng Yue, Yuchen Fan, Yuchen Liang, and Thomas S. Huang. Youtube-vis dataset 2021 version. <https://youtube-vos.org/dataset/vis>, 2021.
- [60] Kaiming He, Georgia Gkioxari, Piotr Dollár, and Ross Girshick. Mask r-cnn. In *Proceedings of the IEEE international conference on computer vision*, pages 2961–2969, 2017.
- [61] Zhi Tian, Chunhua Shen, and Hao Chen. Conditional convolutions for instance segmentation. In *Computer Vision–ECCV 2020: 16th European Conference, Glasgow, UK, August 23–28, 2020, Proceedings, Part I 16*, pages 282–298. Springer, 2020.

A Public Datasets

In this work, we mainly used nine public polyp segmentation datasets, including six image polyp segmentation (IPS) datasets: ClinicDB [29], Kvasir-SEG [32], ColonDB [30], EndoScene [31], ETIS [28] and PS-NBI2K [33], and three video polyp segmentation (VPS) datasets: SUN-SEG [9], PICCOLO [48], PolypGen [49].

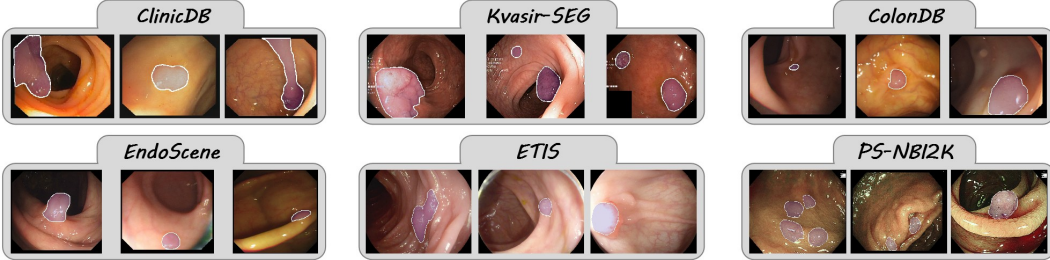
Statistics. We summarize the number of images/frames, videos, and official links for each public dataset in Tab. 7.

Visualization. We select some example cases from each dataset and visualize them in Fig. 5. From it, we find that the IPS datasets contain diverse polyp types, which can enable the segmentation model to learn a more comprehensive polyp contextual knowledge, and thus improve the domain generalization of the polyp segmentation model.

Table 7: Statistics of public/in-house polyp segmentation datasets involved in our work. “#IMG” and “#VID” represents the number of images/frames and videos including in the dataset.

Access	Type	Dataset	#IMG	#VID	URL
Public	IPS	ClinicDB	612	-	Link
		Kvasir-SEG	1,000	-	Link
		ColonDB	380	-	Link
		EndoScene	60	-	Link
		ETIS	196	-	Link
		PS-NBI2K	2,000	-	Link
Public	VPS	SUN-SEG (train)	19,544	112	Link
		SUN-SEG (test)	29,592	173	Link
		PICCOLO	3,433	39	Link
		PolypGen	8,037	23	Link
In-house	VPS	LU-VPS	562,951	15	-

IPS Dataset



VPS Dataset

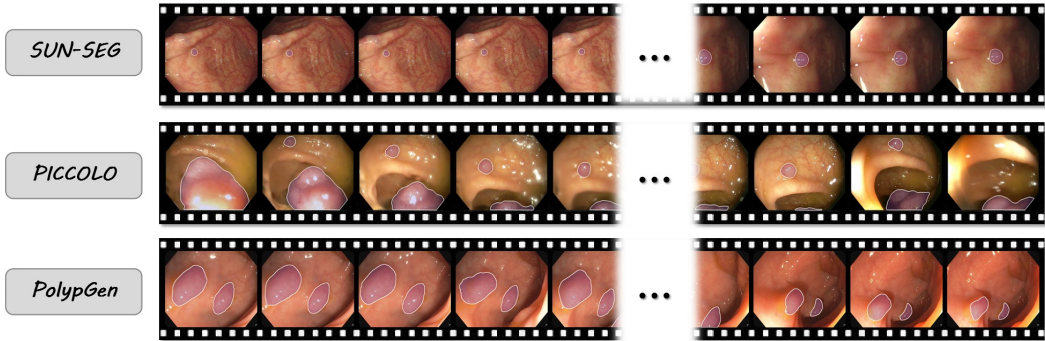


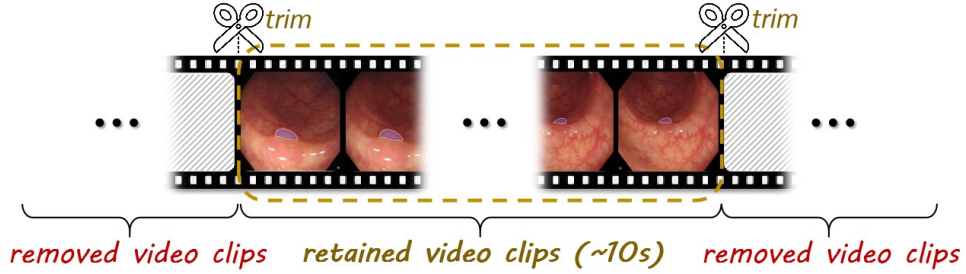
Figure 5: Example cases from the public polyp segmentation datasets, including six IPS datasets and three VPS datasets.

B In-House Dataset: LU-VPS

Existing VPS datasets including the three public video datasets mentioned above (*i.e.*, SUN-SEG, PICCOLO, PolypGen) are all composed of *short-trimmed* video clips, most of which are clips of polyps occurring consecutively. The model’s performance on these datasets can not reflect its performance in real clinical scenarios. To address the limitation, we construct an in-house dataset, namely **LU-VPS**, which contains a total of 9 positive (containing polyps) and 6 negative (without polyps) *long-untrimmed* videos, totaling 562, 951 frames. The length range of each video is 20 ~ 50 minutes, with 15 frames per second (FPS). To more clearly illustrate the difference between the short-trimmed video clips and the long-untrimmed video clips, we show Fig. 6. Furthermore, we cropped a short clip from each video in the LU-VPS dataset and supplemented it in the path “./Sample cases of LU-VPS (In-house Dataset)”.

LU-VPS was collected from a local hospital, with 59, 104 bounding box and 48, 282 pixel-wise mask annotations provided by three endoscopists to support the researchers in testing the detection and segmentation performance of the model. Written informed consent was not required for this study as documented clinical colonoscopic images were collected retrospectively and appropriately by anonymizing and deidentifying. Therefore, the study design was exempted from full review by the Institutional Review Board.

Short-Trimmed VPS Dataset (*e.g.*, SUN-SEG, PICCOLO, PolypGen, ...)



Long-Untrimmed VPS Dataset (Our In-House Dataset: LU-VPS)

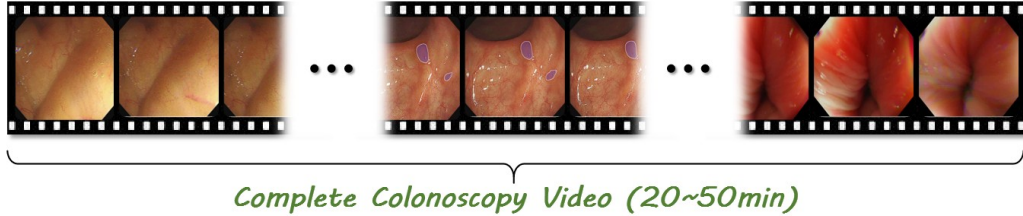


Figure 6: Comparison between existing public short-trimmed VPS datasets and our in-house long-untrimmed VPS dataset.

C Ablation on Two Hyperparameters: λ_1 and λ_2

We conduct an ablation study on SUN-SEG dataset to examine the effect of the values of hyperparameters: λ_1 and λ_1 , which are defined in Sec. 3.3 of manuscript. λ_1 primarily affects the process by which newly discovered polyp instances are added to the SAM2’s memory bank, whereas λ_2 primarily plays a role in the removal of information about disappearing polyps from the memory bank.

As reported in Tab. 8, we can see that FreeVPS with $\lambda_1 = 1$ and $\lambda_2 = 3$ shows the best performance. Therefore, we follow this definition of hyperparameters in FreeVPS by default.

Table 8: Ablation on two hyperparameters: λ_1 and λ_2 .

λ_1	Dice	IoU	MAE	TC	λ_2	Dice	IoU	MAE	TC
1	88.4	82.5	1.6	74.7	1	83.2	74.7	2.7	73.4
2	88.0	81.8	1.5	74.5	2	87.4	80.7	1.8	74.1
3	87.5	81.4	1.8	74.2	3	88.4	82.5	1.6	74.7
4	87.2	81.0	1.8	74.1	4	88.1	82.0	1.6	74.4

Table 9: Verification of FreeVPS’s generality for other image polyp segmentation models.

Methods	SUN-SEG (In Domain)				PICCOLO (Out-of-domain)			
	Dice \uparrow	IoU \uparrow	MAE \downarrow	TC \uparrow	Dice \uparrow	IoU \uparrow	MAE \downarrow	TC \uparrow
Polyp-PVT [26]	80.0	71.9	3.6	69.8	65.1	58.3	8.4	65.5
+ FreeVPS	86.1 _{+6.1}	79.6 _{+7.7}	2.6 _{−1.0}	73.7 _{+3.9}	73.0 _{+7.9}	66.4 _{+8.1}	6.5 _{−1.9}	68.9 _{+3.4}
Polyper [50]	80.8	73.0	3.3	70.3	66.3	59.1	8.2	65.8
+ FreeVPS	86.4 _{+5.6}	80.3 _{+7.3}	2.4 _{−0.9}	74.0 _{+3.7}	74.5 _{+8.2}	67.8 _{+8.7}	6.3 _{−1.9}	69.1 _{+3.3}

D Generality for Other Image Polyp Segmentation Models

FreeVPS is a plug-and-play framework and can improve the performance of any IPS model in VPS task. To verify the generality of FreeVPS, we introduce IPS models, PolypPVT [26] and Polyper [50]. Specifically, we retrain these IPS models using the combined set of \mathcal{D}_V and \mathcal{D}_I , and then test their performance individually and when integrated with our FreeVPS on an in-domain (ID) dataset, SUN-SEG, and an out-of-domain (OOD) dataset, PICCOLO, respectively.

As shown in Tab. 9, we find that FreeVPS improves all metrics of all these IPS models on both ID and OOD datasets, which fully demonstrates the generality of our FreeVPS for various image polyp segmentation models.

E More Visualization Results

To provide a comprehensive visualization of FreeVPS’s performance, we have included supplementary GIFs in the Appendix zip. These dynamic visualizations, which more intuitively demonstrates the superiority of FreeVPS, are organized in the path “./Visualization results in ID and OOD scenarios”.

F Limitations

FreeVPS can adapt a pre-trained IPS model to the video domain in a training-free manner, although this has achieved a lot of success, there are still the following main limitations: (1) FreeVPS still relies on a reliable IPS model, which is a common problem in track-by-detect paradigm. We plan to collect a large-scale polyp dataset (including images and videos) to train a robust colonoscopy-specific foundation model, further enhancing the performance of FreeVPS. (2) The memory refinement mechanism will introduce latency in detecting newly appeared polyps, with a temporal delay of $0 \sim T \cdot \lambda_1$ frames ($T = 3$ and $\lambda_1 = 1$ in our default setting), even though this small delay does not affect the endoscopist’s screening workflow.

G Broader Impacts

FreeVPS achieves a better balance between spatiotemporal modeling and domain generalization compared to existing polyp segmentation methods and shows superior performance on the in-house long-untrimmed VPS dataset, which demonstrates the potential of FreeVPS in assisting clinical colonoscopy. Further advancement in application requires subsequent validation in more rigorous clinical trials. Moreover, FreeVPS eliminates the dependency on video-specific training data and is also expected to address the other medical video tasks where video data is scarce.

NeurIPS Paper Checklist

1. Claims

Question: Do the main claims made in the abstract and introduction accurately reflect the paper's contributions and scope?

Answer: [\[Yes\]](#)

Justification: Our abstract and introduction clearly state main contributions made in the paper. Our experimental results also support our claim.

Guidelines:

- The answer NA means that the abstract and introduction do not include the claims made in the paper.
- The abstract and/or introduction should clearly state the claims made, including the contributions made in the paper and important assumptions and limitations. A No or NA answer to this question will not be perceived well by the reviewers.
- The claims made should match theoretical and experimental results, and reflect how much the results can be expected to generalize to other settings.
- It is fine to include aspirational goals as motivation as long as it is clear that these goals are not attained by the paper.

2. Limitations

Question: Does the paper discuss the limitations of the work performed by the authors?

Answer: [\[Yes\]](#)

Justification: We have a dedicated section to discuss the limitations of our work. Please refer to Appx. F.

Guidelines:

- The answer NA means that the paper has no limitation while the answer No means that the paper has limitations, but those are not discussed in the paper.
- The authors are encouraged to create a separate "Limitations" section in their paper.
- The paper should point out any strong assumptions and how robust the results are to violations of these assumptions (e.g., independence assumptions, noiseless settings, model well-specification, asymptotic approximations only holding locally). The authors should reflect on how these assumptions might be violated in practice and what the implications would be.
- The authors should reflect on the scope of the claims made, e.g., if the approach was only tested on a few datasets or with a few runs. In general, empirical results often depend on implicit assumptions, which should be articulated.
- The authors should reflect on the factors that influence the performance of the approach. For example, a facial recognition algorithm may perform poorly when image resolution is low or images are taken in low lighting. Or a speech-to-text system might not be used reliably to provide closed captions for online lectures because it fails to handle technical jargon.
- The authors should discuss the computational efficiency of the proposed algorithms and how they scale with dataset size.
- If applicable, the authors should discuss possible limitations of their approach to address problems of privacy and fairness.
- While the authors might fear that complete honesty about limitations might be used by reviewers as grounds for rejection, a worse outcome might be that reviewers discover limitations that aren't acknowledged in the paper. The authors should use their best judgment and recognize that individual actions in favor of transparency play an important role in developing norms that preserve the integrity of the community. Reviewers will be specifically instructed to not penalize honesty concerning limitations.

3. Theory assumptions and proofs

Question: For each theoretical result, does the paper provide the full set of assumptions and a complete (and correct) proof?

Answer: [NA]

Justification: The paper does not include theoretical results.

Guidelines:

- The answer NA means that the paper does not include theoretical results.
- All the theorems, formulas, and proofs in the paper should be numbered and cross-referenced.
- All assumptions should be clearly stated or referenced in the statement of any theorems.
- The proofs can either appear in the main paper or the supplemental material, but if they appear in the supplemental material, the authors are encouraged to provide a short proof sketch to provide intuition.
- Inversely, any informal proof provided in the core of the paper should be complemented by formal proofs provided in appendix or supplemental material.
- Theorems and Lemmas that the proof relies upon should be properly referenced.

4. Experimental result reproducibility

Question: Does the paper fully disclose all the information needed to reproduce the main experimental results of the paper to the extent that it affects the main claims and/or conclusions of the paper (regardless of whether the code and data are provided or not)?

Answer: [Yes]

Justification: The proposed model is described in Section 3. The detailed training setting and experimental setup are given in Section 4.2. All training datasets in this work are open-source and accessible. The trained model and code will be released after the review period.

Guidelines:

- The answer NA means that the paper does not include experiments.
- If the paper includes experiments, a No answer to this question will not be perceived well by the reviewers: Making the paper reproducible is important, regardless of whether the code and data are provided or not.
- If the contribution is a dataset and/or model, the authors should describe the steps taken to make their results reproducible or verifiable.
- Depending on the contribution, reproducibility can be accomplished in various ways. For example, if the contribution is a novel architecture, describing the architecture fully might suffice, or if the contribution is a specific model and empirical evaluation, it may be necessary to either make it possible for others to replicate the model with the same dataset, or provide access to the model. In general, releasing code and data is often one good way to accomplish this, but reproducibility can also be provided via detailed instructions for how to replicate the results, access to a hosted model (e.g., in the case of a large language model), releasing of a model checkpoint, or other means that are appropriate to the research performed.
- While NeurIPS does not require releasing code, the conference does require all submissions to provide some reasonable avenue for reproducibility, which may depend on the nature of the contribution. For example
 - (a) If the contribution is primarily a new algorithm, the paper should make it clear how to reproduce that algorithm.
 - (b) If the contribution is primarily a new model architecture, the paper should describe the architecture clearly and fully.
 - (c) If the contribution is a new model (e.g., a large language model), then there should either be a way to access this model for reproducing the results or a way to reproduce the model (e.g., with an open-source dataset or instructions for how to construct the dataset).
 - (d) We recognize that reproducibility may be tricky in some cases, in which case authors are welcome to describe the particular way they provide for reproducibility. In the case of closed-source models, it may be that access to the model is limited in some way (e.g., to registered users), but it should be possible for other researchers to have some path to reproducing or verifying the results.

5. Open access to data and code

Question: Does the paper provide open access to the data and code, with sufficient instructions to faithfully reproduce the main experimental results, as described in supplemental material?

Answer: [Yes]

Justification: All of the datasets involved in this work are open-source and accessible, except one in-house dataset for evaluating zero-shot generalization. The detailed descriptions of these datasets are presented in Section 4.1 and Appx. B. The trained model and code will be released after the review period.

Guidelines:

- The answer NA means that paper does not include experiments requiring code.
- Please see the NeurIPS code and data submission guidelines (<https://nips.cc/public/guides/CodeSubmissionPolicy>) for more details.
- While we encourage the release of code and data, we understand that this might not be possible, so “No” is an acceptable answer. Papers cannot be rejected simply for not including code, unless this is central to the contribution (e.g., for a new open-source benchmark).
- The instructions should contain the exact command and environment needed to run to reproduce the results. See the NeurIPS code and data submission guidelines (<https://nips.cc/public/guides/CodeSubmissionPolicy>) for more details.
- The authors should provide instructions on data access and preparation, including how to access the raw data, preprocessed data, intermediate data, and generated data, etc.
- The authors should provide scripts to reproduce all experimental results for the new proposed method and baselines. If only a subset of experiments are reproducible, they should state which ones are omitted from the script and why.
- At submission time, to preserve anonymity, the authors should release anonymized versions (if applicable).
- Providing as much information as possible in supplemental material (appended to the paper) is recommended, but including URLs to data and code is permitted.

6. Experimental setting/details

Question: Does the paper specify all the training and test details (e.g., data splits, hyper-parameters, how they were chosen, type of optimizer, etc.) necessary to understand the results?

Answer: [Yes]

Justification: The detailed experiment setting is described in Section 4.2. The trained model and code will be released after the review period.

Guidelines:

- The answer NA means that the paper does not include experiments.
- The experimental setting should be presented in the core of the paper to a level of detail that is necessary to appreciate the results and make sense of them.
- The full details can be provided either with the code, in appendix, or as supplemental material.

7. Experiment statistical significance

Question: Does the paper report error bars suitably and correctly defined or other appropriate information about the statistical significance of the experiments?

Answer: [No]

Justification: We follow the common practice in prior works and report the performance number on the standard benchmarks.

Guidelines:

- The answer NA means that the paper does not include experiments.

- The authors should answer "Yes" if the results are accompanied by error bars, confidence intervals, or statistical significance tests, at least for the experiments that support the main claims of the paper.
- The factors of variability that the error bars are capturing should be clearly stated (for example, train/test split, initialization, random drawing of some parameter, or overall run with given experimental conditions).
- The method for calculating the error bars should be explained (closed form formula, call to a library function, bootstrap, etc.)
- The assumptions made should be given (e.g., Normally distributed errors).
- It should be clear whether the error bar is the standard deviation or the standard error of the mean.
- It is OK to report 1-sigma error bars, but one should state it. The authors should preferably report a 2-sigma error bar than state that they have a 96% CI, if the hypothesis of Normality of errors is not verified.
- For asymmetric distributions, the authors should be careful not to show in tables or figures symmetric error bars that would yield results that are out of range (e.g. negative error rates).
- If error bars are reported in tables or plots, The authors should explain in the text how they were calculated and reference the corresponding figures or tables in the text.

8. Experiments compute resources

Question: For each experiment, does the paper provide sufficient information on the computer resources (type of compute workers, memory, time of execution) needed to reproduce the experiments?

Answer: [Yes]

Justification: The information on computer resources is provided in Section 4.2.

Guidelines:

- The answer NA means that the paper does not include experiments.
- The paper should indicate the type of compute workers CPU or GPU, internal cluster, or cloud provider, including relevant memory and storage.
- The paper should provide the amount of compute required for each of the individual experimental runs as well as estimate the total compute.
- The paper should disclose whether the full research project required more compute than the experiments reported in the paper (e.g., preliminary or failed experiments that didn't make it into the paper).

9. Code of ethics

Question: Does the research conducted in the paper conform, in every respect, with the NeurIPS Code of Ethics <https://neurips.cc/public/EthicsGuidelines>?

Answer: [Yes]

Justification: Research conducted in the paper conforms with the NeurIPS Code of Ethics.

Guidelines:

- The answer NA means that the authors have not reviewed the NeurIPS Code of Ethics.
- If the authors answer No, they should explain the special circumstances that require a deviation from the Code of Ethics.
- The authors should make sure to preserve anonymity (e.g., if there is a special consideration due to laws or regulations in their jurisdiction).

10. Broader impacts

Question: Does the paper discuss both potential positive societal impacts and negative societal impacts of the work performed?

Answer: [Yes]

Justification: We have a dedicated section to discuss the societal impacts of our work. Please refer to Appx. G.

Guidelines:

- The answer NA means that there is no societal impact of the work performed.
- If the authors answer NA or No, they should explain why their work has no societal impact or why the paper does not address societal impact.
- Examples of negative societal impacts include potential malicious or unintended uses (e.g., disinformation, generating fake profiles, surveillance), fairness considerations (e.g., deployment of technologies that could make decisions that unfairly impact specific groups), privacy considerations, and security considerations.
- The conference expects that many papers will be foundational research and not tied to particular applications, let alone deployments. However, if there is a direct path to any negative applications, the authors should point it out. For example, it is legitimate to point out that an improvement in the quality of generative models could be used to generate deepfakes for disinformation. On the other hand, it is not needed to point out that a generic algorithm for optimizing neural networks could enable people to train models that generate Deepfakes faster.
- The authors should consider possible harms that could arise when the technology is being used as intended and functioning correctly, harms that could arise when the technology is being used as intended but gives incorrect results, and harms following from (intentional or unintentional) misuse of the technology.
- If there are negative societal impacts, the authors could also discuss possible mitigation strategies (e.g., gated release of models, providing defenses in addition to attacks, mechanisms for monitoring misuse, mechanisms to monitor how a system learns from feedback over time, improving the efficiency and accessibility of ML).

11. Safeguards

Question: Does the paper describe safeguards that have been put in place for responsible release of data or models that have a high risk for misuse (e.g., pretrained language models, image generators, or scraped datasets)?

Answer: [NA]

Justification: Our work does not pose such risks to the best of our knowledge.

Guidelines:

- The answer NA means that the paper poses no such risks.
- Released models that have a high risk for misuse or dual-use should be released with necessary safeguards to allow for controlled use of the model, for example by requiring that users adhere to usage guidelines or restrictions to access the model or implementing safety filters.
- Datasets that have been scraped from the Internet could pose safety risks. The authors should describe how they avoided releasing unsafe images.
- We recognize that providing effective safeguards is challenging, and many papers do not require this, but we encourage authors to take this into account and make a best faith effort.

12. Licenses for existing assets

Question: Are the creators or original owners of assets (e.g., code, data, models), used in the paper, properly credited and are the license and terms of use explicitly mentioned and properly respected?

Answer: [Yes]

Justification: We properly credited the creators or original owners of assets (e.g., code, data, models), used in the paper and conformed the license and terms.

Guidelines:

- The answer NA means that the paper does not use existing assets.
- The authors should cite the original paper that produced the code package or dataset.
- The authors should state which version of the asset is used and, if possible, include a URL.
- The name of the license (e.g., CC-BY 4.0) should be included for each asset.

- For scraped data from a particular source (e.g., website), the copyright and terms of service of that source should be provided.
- If assets are released, the license, copyright information, and terms of use in the package should be provided. For popular datasets, paperswithcode.com/datasets has curated licenses for some datasets. Their licensing guide can help determine the license of a dataset.
- For existing datasets that are re-packaged, both the original license and the license of the derived asset (if it has changed) should be provided.
- If this information is not available online, the authors are encouraged to reach out to the asset's creators.

13. **New assets**

Question: Are new assets introduced in the paper well documented and is the documentation provided alongside the assets?

Answer: [Yes]

Justification: Our new assets introduced in the paper are well documented in the Section 4.1 and Appx. B.

Guidelines:

- The answer NA means that the paper does not release new assets.
- Researchers should communicate the details of the dataset/code/model as part of their submissions via structured templates. This includes details about training, license, limitations, etc.
- The paper should discuss whether and how consent was obtained from people whose asset is used.
- At submission time, remember to anonymize your assets (if applicable). You can either create an anonymized URL or include an anonymized zip file.

14. **Crowdsourcing and research with human subjects**

Question: For crowdsourcing experiments and research with human subjects, does the paper include the full text of instructions given to participants and screenshots, if applicable, as well as details about compensation (if any)?

Answer: [NA]

Justification: Our research does not involve crowdsourcing nor research with human subjects.

Guidelines:

- The answer NA means that the paper does not involve crowdsourcing nor research with human subjects.
- Including this information in the supplemental material is fine, but if the main contribution of the paper involves human subjects, then as much detail as possible should be included in the main paper.
- According to the NeurIPS Code of Ethics, workers involved in data collection, curation, or other labor should be paid at least the minimum wage in the country of the data collector.

15. **Institutional review board (IRB) approvals or equivalent for research with human subjects**

Question: Does the paper describe potential risks incurred by study participants, whether such risks were disclosed to the subjects, and whether Institutional Review Board (IRB) approvals (or an equivalent approval/review based on the requirements of your country or institution) were obtained?

Answer: [NA]

Justification: Our research does not involve crowdsourcing nor research with human subjects.

Guidelines:

- The answer NA means that the paper does not involve crowdsourcing nor research with human subjects.

- Depending on the country in which research is conducted, IRB approval (or equivalent) may be required for any human subjects research. If you obtained IRB approval, you should clearly state this in the paper.
- We recognize that the procedures for this may vary significantly between institutions and locations, and we expect authors to adhere to the NeurIPS Code of Ethics and the guidelines for their institution.
- For initial submissions, do not include any information that would break anonymity (if applicable), such as the institution conducting the review.

16. **Declaration of LLM usage**

Question: Does the paper describe the usage of LLMs if it is an important, original, or non-standard component of the core methods in this research? Note that if the LLM is used only for writing, editing, or formatting purposes and does not impact the core methodology, scientific rigorousness, or originality of the research, declaration is not required.

Answer: [NA]

Justification: Our research does not involve LLMs as any important, original, or non-standard components.

Guidelines:

- The answer NA means that the core method development in this research does not involve LLMs as any important, original, or non-standard components.
- Please refer to our LLM policy (<https://neurips.cc/Conferences/2025/LLM>) for what should or should not be described.